HHS Public Access

Author manuscript

Cornea. Author manuscript; available in PMC 2021 September 01.

Published in final edited form as:

Cornea. 2020 September ; 39(9): 1145–1150. doi:10.1097/ICO.0000000000002371.

Ocular manifestations of chordin-like 1 knockout mice

Di Chen, MD[1,2], **Yang Liu, MD**[2], **Guanhua Shu, MS**[3], **Chinfei Chen, PhD**[3], **David A. Sullivan, PhD**[2], **Wendy R. Kam, MS**[2], **Steven Hann, PhD**[4], **Megan Fowler, BS**[4], **Matthew L. Warman, PhD**[4]

[1]Department of Ophthalmology, Peking Union Medical College Hospital, Chinese Academy of Medical Sciences & Peking Union Medical College, Beijing, China;

[2]Schepens Eye Research Institute, Massachusetts Eye and Ear, and Department of Ophthalmology, Harvard Medical School, Boston, MA, USA;

[3]F.M. Kirby Neurobiology Center, Boston Children's Hospital, Harvard Medical School, Boston, MA 02115

[4]Orthopaedic Research Laboratories, Department of Orthopaedic Surgery, Boston Children's Hospital, and Department of Genetics, Harvard Medical School, Boston, MA, USA

Abstract

Purpose.—In humans, loss-of-function mutations in the gene encoding Chordin-like 1 (*CHRDL1*) cause X-linked megalocornea (MGC1), characterized by bilateral corneal enlargement, decreased cornea thickness, and increased anterior chamber depth (ACD). We sought to determine whether *Chrdl1* knockout (KO) mice would recapitulate the ocular findings found in patients with MGC1.

Methods.—We generated mice with a *Chrdl1* knockout allele and confirmed that male *Chrdl1* hemizygous KO mice do not express *Chrdl1* mRNA. We examined the eyes of male mice that were hemizygous for either the wild-type (WT) or KO allele and measured corneal diameter, corneal area, corneal thickness, endothelial cell density, ACD, tear volume, and intraocular pressure. We also harvested retinas and counted retinal ganglion cell numbers. Eye segregation pattern in the dorsal lateral geniculate nucleus were also compared between male *Chrdl1* KO and WT mice.

Results.—Male *Chrdl1* KO mice do not have larger cornea diameters than WT mice. KO mice have significantly thicker central corneas (116.5 ± 3.9 vs 100.9 ± 4.2 μm, $p = 0.013$) and smaller ACD (325.7 ± 5.7 vs 405.6 ± 6.3 μm, $p < 0.001$) than WT mice, which is the converse of what occurs in patients who lack CHRDL1. Retinal- thalamic projections and other ocular measurements did not significantly differ between KO and WT mice.

Conclusions.—Male *Chrdl1* KO mice do not have the same anterior chamber abnormalities seen in humans with *CHRDL1* mutations. Therefore, *Chrdl1* KO mice do not recapitulate the

Corresponding Author: Di Chen, MD, Department of Ophthalmology, Peking Union Medical College Hospital, No.1 Shuaifuyuan Road, Dongcheng District, Beijing, China 100730, chendi@pumch.cn.

Conflicts of interest: All of the authors declare no conflicts of interests.

human MGC1 phenotype. Nevertheless, *Chrdl1* plays a role during mouse ocular development, since corneas in KO mice differ from those in WT mice.

Keywords

megalocornea; Chordin-like 1; ocular manifestations; gene knockout mice; cornea diameter

Introduction

X-linked megalocornea (MGC1; OMIM 309300) is a heritable disorder that affects the anterior segment of the eye. Males with MGC1 have increased cornea diameters, thin central corneas, and deep anterior chambers[1]. With aging, mosaic corneal degeneration (shagreen) and corneal arcus juvenilis, mild iris atrophy with pigment dispersion, lens dislocation, and cataracts can occur[2,3]. MGC1 is caused by hemizygous loss-of-function mutations in Chordin-like 1 *(CHRDL1)*[4,5], which is also known as ventropin, neuralin-1, and neurogenesin-1. *Ex vivo* and transient *in vivo* knockdown and/or overexpression studies using cells, frog larvae, and chick embyros, indicate Chordin-like 1 may function as an extracellular antagonist to bone morphogenetic protein (BMP) signaling[4,6–8].

In order to determine whether Chordin-like 1 function is evolutionarily conserved in mice, we examined the ocular phenotype of male *Chrdl1* knockout (KO) mice. Surprisingly, KO mice do not recapitulate the ocular features found in human patients.

Materials and Methods

Experimental Animals

We obtained a 129S5 embryonic stem (ES) cell line (UTT092) created by Lexicon Pharmaceuticals (The Woodlands, TX) in which the first coding exon of *Chrdl1* was mutated by homologous recombination (see supplementary information). We used this ES line to generate mice having a mixed 129S5/C57BL6J background. We crossed female mice that were heterozygous for *Chrdl1* KO allele with wild-type (WT) males and studied only the male offspring. Male offspring were either hemizygous for a KO or WT allele. We compared male WT and KO littermates, when possible. Otherwise, male WT and KO offspring from different litters were compared. All experiments were approved by the Institutional Animal Care and Use Committees of Boston Children's Hospital and the Schepens Eye Research Institute, and adhered to the Association for Research in Vision and Ophthalmology Statement for the Use of Animals in Ophthalmic and Vision Research.

Genotyping and Reverse Transcription Polymerase Chain Reactions (RT-PCR)

DNA for genotyping was obtained and extracted from tail biopsies using standard methods. Two separate PCR reactions distinguished WT from KO alleles. Primer pair C1KO-F and C1KOWTR (5' – TTCGCTCCACTACATTCTCC and 5' – CATGAACATGGCCACATTTGG, respectively) produced a 374 bp amplimer in WT males, and primer pair C1KO-MFJ and C1KO-MRJ (5' – AAGGCCGGTGTGCGTTTGTCT and 5' – ACACGTGGCTTTGGCCGCA, respectively) produced a 267 bp amplimer in KO males. Because *Chrdl1* expression in kidney has been previously described in the Mouse

Genome Informatics database (informatics.jax.org) and in the Genotype-Tissue Expression database (gtexportal.org), we extracted RNA from male WT and KO mouse kidneys for RT-PCR. RNA was converted to cDNA using standard methods. A primer pair spanning the exon 6/7 splice junction (5' – GCTGCCGAGTATGCAGAGGGG) and the 3'UTR in exon 12 (5' – TTGGAGCGCTGCAGCTTGGG) of *Chrdl1* variant 1 produces an 894 bp amplimer from WT *Chrdl1* cDNA. A primer pair spanning the exon 6/7 splice junction and the 3'UTR after exon 9 (5' - CCAAAGGCAGGGCCTCCAGC) of *Chdrl1* variant 2 produces a 492 bp amplimer from wild-type *Chrdl1* cDNA. As a positive control for RT-PCR we used a primer pair Tuba1a-F and Tuba1a-R (5' - AGCAGCAACCATGCGTGA and 5' - CAGGTCTACGAACACTGCCC, respectively) that produces a 216 bp amplimer from a spliced mRNA transcript encoding alpha tubulin (*Tuba1a*).

Corneal Fluorescein Staining (CFS)

Corneal fluorescein staining was evaluated by applying 1 μL of 5% fluorescein (Ful-Glo; Akorn Pharmaceuticals, Lake Forest, IL) by micropipette into the inferior conjunctival sac of both eyes of the mice. The cornea was examined with a slit lamp biomicroscope in cobalt blue light. Punctuate staining was recorded in a masked fashion with National Eye Institute (NEI) grading system with a range of 0 to 15[9].

Tear Volume Measurement

Phenol red threads (Zone-Quick; Lacrimedics, Eastsound, WA) were applied to measure the tear volume as described[10]. In brief, the threads were placed in the lateral canthus of the eye for 30 seconds after the removal of excess tears. Tear distance was then determined with the manufacturer-supplied scale.

Intraocular Pressure (IOP) Measurement

We employed a published protocol to measure the IOP[11]. A TonoLab tonometer (Icare, Tampere, Finland) was used to measure IOP (n = 6 consecutive measurements per IOP value, 3 values per eye) at the central cornea of conscious mice secured in DecapiCone bags. Measurements of the IOP were performed in a masked fashion between 10 and 11 AM.

Cornea Endothelial Cell Density

To assess corneal endothelial density, mice were deeply anesthetized with an intraperitoneal injection of ketamine (200 mg/kg) /xylazine (20 mg/kg) and we used a Heidelberg Retina Tomograph (HRT II, Heidelberg Engineering, Heidelberg, Germany) equipped with a Rostock Cornea Module (RCM, Heidelberg Engineering, Heidelberg, Germany). A PMMA (polymethyl methacrylate) cap was connected via contact gel (Genteal, Alcon Laboratories, Fort Worth, TX) to the immersion objective and cornea. The image size was 300 × 300 μm with a vertical optical resolution of 2 μm. The endothelial cells were marked and counted in a predetermined image area through HRT associated cell count software to achieve the cornea endothelial cell density. The cells touching the border lines were counted only along the left and lower borders.

Anterior Segment Optical Coherence Tomography (AS-OCT)

To examine the anterior segment, we utilized a spectral-domain optical coherence tomography system (Bioptigen, Morrisville, NC). The system was fitted with an additional corneal lens adapter (cornea anterior module-low magnification) to provide a scan length of 2 to 6 mm and an image size of 12 × 8 mm. After anesthesia, the mice were restrained in a mounting tube that was fixed on a six-axis platform. Genteal gel was applied to both eyes to prevent drying of the cornea. The alignment was guided manually to ensure that scans were centered on the pupil and taken along the horizontal axis (nasal-temporal angles at 0–180°). The set up procedure took approximately 5 minutes for each mouse eye. The InVivoVue Clinic, in the Bioptigen Software, was used to perform real-time data acquisition, processing, archiving, and display. Central corneal thickness (CCT) and anterior chamber depth (ACD) were measured along the vertical line orthogonal to the anterior corneal curvature and passing through the center of the pupil. CCT was defined as the distance from the corneal epithelium to endothelium along this line and ACD was measured from the corneal endothelium to the anterior surface of the crystalline lens as described.[12,13] The corneal diameter was measured by using the visualized corneoscleral junction to define the limit of the cornea on the image taken from the OCT.

For the above procedures, the CFS, tear volume and IOP measurements were performed without anesthesia on different days. The evaluation of AS-OCT and then cornea endothelial cell density was conducted under anesthesia on the same day.

Cornea Area Measurement

At the termination of experiments, the mice were euthanized by CO_2 inhalation and the eyes were carefully enucleated. Corneal images were immediately obtained under a dissecting microscope (Stereo Star, American Optical, Southbridge, MA) at a fixed magnification (×20) and position. The whole cornea area was outlined by the corneoscleral junction and measured with ImageJ (https://imagej.nih.gov/ij/index.html).

Retinal Ganglion Cell (RGC) Counting

The RGC count was quantitated as described[11,14]. In brief, the euthanized mice were immediately perfused intracardially with phosphate-buffered saline (PBS). Eyes were removed, fixed and processed for the preparation of retinal flat mounts (cut into 4 quadrants). Retinal samples were incubated with mouse anti-mouse Brn3a antibody (Millipore Sigma, Burlington, MA; diluted 1:200 in blocking buffer [2% bovine serum albumin and 2% Triton]) overnight at 4 °C, and then exposed to donkey anti-mouse IgG antibody (Millipore; diluted 1:200 in blocking buffer) for 2 hours at room temperature. Samples were then mounted and RGCs were imaged with a confocal microscope (Leica TCS SP5 CLSM, zoom = 800-fold). RGCs were counted manually in 3 random areas along the centerline of each quadrant (total = 3 counts/quadrant, 12 counts/retina).

Intravitreal injections

To compare the eye segregation pattern in the dorsal lateral geniculate nucleus (dLGN) of *Chrdl1* KO and WT mice, Cholera Toxin Subunit B (CTB) (Millipore Sigma, # C9903) conjugated with Alexa 488 or 594 was injected into left and right eye, respectively. A

Hamilton syringe (Hamilton company, Reno, NV) loaded with CTB was inserted into the vitreous humor space of each eye and CTB (1.5 μl) slowly injected over about 1 minute. After waiting 48 hours to allow the CTB to be taken up into retinal ganglion cells and transported down their axons, the animals were sacrificed and tissues fixed by transcardial perfusion. The mice used in these studies were different than those utilized for the anterior segment analyses.

Brain Slicing and Image Acquisition

Mice were anesthetized with intraperitoneal injection of pentobarbital (100 mg/kg, diluted in saline). A thoracotomy was then performed and the heart of the animal exposed. A syringe with a 27-gauge needle was inserted into the left ventricle and the right ventricle was incised to allow for drainage. Ten to 20ml 1X PBS was slowly injected to clear the blood, followed by 10–15ml 4% paraformaldehyde. Harvested brains and eyeballs were then placed in a 4% paraformaldehyde solution overnight at 4 °C. After 24 hours, 4% paraformaldehyde containing brain tissue and eyeballs was replaced with 1X PBS for long-term storage.

Fixed brain tissues were sliced using a vibratome (Leica Microsystems, Wetzlar, Germany) and 65μm thick brain sections were prepared. Sections that contain the dorsal lateral geniculate nucleus (dLGN) were selected and mounted with mounting medium (Vector Laboratories, Burlingame, CA; H-1000). Mounted brain sections and retinas were imaged using an epifluorescence microscope (Nikon 80i air, Nikon Instruments, Melville, NY) with 4x objective.

ImageJ Analysis and Mean R Variance Analysis

dLGN images were analyzed using ImageJ and a custom written macro (Matlab, Mathworks, Natick, MA) to calculate the mean R variance as described by Torborg and Feller[15]. Briefly, the R ratio is calculated as $\log_{10}(F_I / F_C)$ where F_I corresponds to the pixel fluorescence intensity from ipsilateral eye and F_C represents fluorescence intensity from contralateral eye. A positive R ratio value indicates that fluorescence from ipsilateral retinal projections dominate whereas a negative value indicates contralateral retinal projections dominate. The R variance was calculated by calculating the variance of R ratios of all pixels within a dLGN section and the mean R variance was averaged over multiple dLGN image sections that come from each *Chrdl1* genotype.

Statistical Analysis

All statistical analyses were performed with Prism 7 (GraphPad Software, Inc., La Jolla, CA). Normality of the data was tested by Shapiro-Wilk test. For normally distributed data, values were provided as mean ± standard error and comparisons were performed with two-tailed Student's t-tests. For data that were not normally distributed, values were presented as median (range) and comparisons were made with Mann-Whitney U test. $P < 0.05$ was considered significant.

Results

Experimental Animal Confirmation

The ES cell line UTT092 was used to generate hemizygous male Chrdl1 KO mice (Figure 1). These mice lack the portion exon 2 that contains the ATG translation initiation site and encodes the protein's signal peptide There is no evidence in public databases (e.g., gtexportal.org and genome.ucsc.edu) that *Chrdl1* has alternative transcription or translation start sites. Therefore, disruption exon 2 is predicted to eliminate *Chrdl1* mRNA expression. We tested for the expression of *Chrdl1* by performing RT-PCR.. Whereas kidney mRNA from a WT male yielded 894 bp and 492 bp amplimers after RT-PCR for *Chrdl1* variants 1 and 2, respectively, no amplimer was produced from a KO male (Figure 1).

Ocular Parameters

Having demonstrated that KO males do not express *Chrdl1* mRNA, we next examined the ocular phenotype in 5.5 ± 0.8-month-old KO males (n = 8) and in 8.7 ± 0.6-month-old WT males (N = 7). We only examined male mice because MGC1 is an X-linked recessive human phenotype.

We did not observe increased corneal diameter, corneal thinning, or increased ACD in the KO mice (Table 1 and Figure 2). Instead, KO mice had significantly thicker corneas ($p < 0.05$) and shallower anterior chambers ($p < 0.001$) than WT mice (Figure 3). Lack of *Chrdl1* expression had no significant effect on the tear volume, corneal fluorescein staining, corneal endothelial cell morphology and density, IOP or RGC number (Table 1).

Eye Segregation Pattern

It has been suggested, based on the dorsal ventral gradient of *Chrdl1* expression in developing chick retinas, that CHRDL1 might play a role in guiding projections from the retina to their brain targets[7]. To assess eye-specific segregation of retinal axons in the dorsal lateral geniculate nucleus (dLGN), we injected each eye with different fluorescent label in male KO and WT mice. The left eye was injected with cholera toxin subunit B (CTB) labeled with Alexa 488 (green) and right eye with CTB Alexa 594 (red). Figure 4A shows representative examples of the labeled axons in the dLGN. In WT mice, a clear eye segregation pattern was displayed with a small ipsilateral termination zone in the dorsal medial region surrounded by a much larger contralateral termination area. No gross difference in segregation was obvious in dLGNs of KO compared to WT littermates (Figure 4B).

To measure eye segregation pattern quantitatively, we compared the R ratio and mean R variance of KO and WT images. R ratio defines the relationship between fluorescence intensity from the red and green channels at each pixel. A pixel R ratio approaching zero suggests that approximately equal amounts of fluorescently labeled axons from both ipsilateral and contralateral retina are present at that point in dLGN space. Any deviation from 0 indicates that the pixel contains axons that predominately come from one or the other eye. Mean R variance was not significantly different when comparing KO (n = 18 sections) to WT (n =15 sections; $P > 0.05$) (Figure 4C). We also analyzed mean R variance by mouse

(n = 4 KO, n = 3 WT; $P > 0.05$) and saw no significant difference (data not shown). Therefore, male *Chrdl1* KO mice do not exhibit a defect in retinal axon mapping in the dLGN.

Discussion

Although many developmental pathways exhibit conservation across species, the effect of *Chrdl1* deficiency in mice does not recapitulate that which occurs in humans. Whereas, MGC1 in humans is characterized by significantly increased corneal diameter, this measurement is normal in *Chrdl1* KO mice. Furthermore, KO mice exhibit central corneal thickening and decreased anterior chamber depth, which is opposite to that observed in patients with MGC1. Therefore, even though *Chrdl1* deficiency has some effects on ocular development in male mice, these effects are not the same as those occurring in humans.

Developmental differences between human and mouse eyes may explain why mice do not recapitulate the human MGC1 phenotype. The anterior chamber and lens in mice comprise a much larger fraction of the total eye volume than in humans. Also, whereas human corneal thickness increases from the central area to the periphery, the opposite occurs in mice[16].

The initial report on the role of *Chrdl1 (*ventroptin) in the chick retina showed that misexpression of the protein disrupted axon mapping in the tectum, secondary to an abnormal expression of ephrin A2 in the retina[7]. As Pfeiffenberger and colleagues showed that disruption of ephrins, including ephrin A2, results in substantial aberrant retinal axon mapping and eye specific mapping in the dLGN, it was reasonable to see if there are gross changes in eye specific segregation in dLGN[17]. Results from our studies did not show gross disruption in the mapping of retinal axons to their retinotopic target in the visual thalamus (dLGN) at P32, an age when this developmental process is thought to be complete. It is important to note that the original chick experiments were misexpression and not KO of *Chrdl1*[7]. When we misexpressed *Chrdl1* in developing chick limbs, we caused limb reduction defects[8]; yet, neither mice nor humans lacking CHRDL1 have limb anomalies. Although we cannot fully exclude subtle defects in retinal patterning in *Chrdl1* KO mice, our results support the idea of distinct roles for *Chrdl1* in different species.

A limitation of our study is that we did not perfectly match the ages of our KO and WT mice. Both cohorts of mice were skeletally and reproductively mature; however, the KO mice were, on average 3 months younger, and it is possible that their ocular phenotype may have evolved over time. This seems unlikely, since young boys with MGC1 already have abnormal corneal diameters and anterior chamber depths. Another limitation is that we generated the mice with the C57BL6J background. We cannot exclude the possibility that genetic background might have certain contribution to the *Chrdl1* expression in mice. Further studies with mice of other genetic backgrounds might be necessary to rule out this possibility.

In conclusion, *Chrdl1* KO mice may not model human MGC1 but may still have utility in deciphering aspects of corneal and retinal development that were not addressed in this study.

Supplementary Material

Refer to Web version on PubMed Central for supplementary material.

Acknowledgments:

The authors thank Dr. Justin Allen for initially characterizing the *Chrdl1* KO mouse strain and for setting up the genotyping assay.

Disclosure of funding: These studies were supported by NIH grants R01AR053237 and R01AR064231 (to M.L.W), R01EY013613 and U54 HD090255 (to C.C.), and National Eye Institute Core Grant P30EY003790, as well as the One Hundred Talent Scholarship Program of Peking Union Medical College Hospital (D.C.), the Margaret S. Sinon Scholar in Ocular Surface Research fund (D.A.S.) and the David A. Sullivan laboratory fund.

Abbreviations:

MGC1	megalocornea
CHRDL1	Chordin-like 1
WT	wild type
KO	knockout
ES	embryonic stem
RT-PCR	polymerase chain reactions
CFS	corneal fluorescein staining
IOP	intraocular pressure
AS-OCT	anterior segment optical coherence tomography
CCT	central corneal thickness
ACD	anterior chamber depth
RGC	retinal ganglion cell
PBS	phosphate-buffered saline
CTB	cholera toxin subunit B
dLGN	dorsal lateral geniculate nucleus

References

1. Han J, Young JW, Frausto RF, et al. X-linked Megalocornea Associated with the Novel CHRDL1 Gene Mutation p.(Pro56Leu*8). Ophthalmic Genet. 2015;36:145–148. [PubMed: 24073597]
2. Mackey DA, Buttery RG, Wise GM, et al. Description of X-linked megalocornea with identification of the gene locus. Arch Ophthalmol. 1991;109:829–833. [PubMed: 2043071]
3. Meire FM, Delleman JW. Biometry in X linked megalocornea: pathognomonic findings. Br J Ophthalmol. 1994;78:781–785. [PubMed: 7803356]

4. Webb TR, Matarin M, Gardner JC, et al. X-linked megalocornea caused by mutations in CHRDL1 identifies an essential role for ventroptin in anterior segment development. Am J Hum Genet. 2012;90:247–259. [PubMed: 22284829]
5. Davidson AE, Cheong SS, Hysi PG, et al. Association of CHRDL1 mutations and variants with X-linked megalocornea, Neuhauser syndrome and central corneal thickness. PLoS One 2014;9:e104163. [PubMed: 25093588]
6. Coffinier C, Tran U, Larrain J, et al. Neuralin-1 is a novel Chordin-related molecule expressed in the mouse neural plate. Mech Dev. 2001;100:119–122. [PubMed: 11118896]
7. Sakuta H, Suzuki R, Takahashi H, et al. Ventroptin: a BMP-4 antagonist expressed in a double-gradient pattern in the retina. Science. 2001;293:111–115. [PubMed: 11441185]
8. Allen JM, McGlinn E, Hill A, et al. Autopodial development is selectively impaired by misexpression of chordin-like 1 in the chick limb. Dev Biol. 2013;381:159–169. [PubMed: 23764427]
9. Lemp MA. Report of the National Eye Institute/Industry workshop on Clinical Trials in Dry Eyes. The CLAO journal : official publication of the Contact Lens Association of Ophthalmologists, Inc. 1995;21:221–232.
10. Dursun D, Wang M, Monroy D, et al. A mouse model of keratoconjunctivitis sicca. Investigative ophthalmology & visual science. 2002;43:632–638. [PubMed: 11867577]
11. Chen X, Liu Y, Zhang Y, et al. Impact of aromatase absence on murine intraocular pressure and retinal ganglion cells. Sci Rep. 2018;8:3280. [PubMed: 29459742]
12. Ho H, Htoon HM, Yam GH, et al. Altered Anterior Segment Biometric Parameters in Mice Deficient in SPARC. Investigative ophthalmology & visual science. 2017;58:386–393. [PubMed: 28122087]
13. Puk O, Dalke C, Favor J, et al. Variations of eye size parameters among different strains of mice. Mamm Genome. 2006;17:851–857. [PubMed: 16897341]
14. Mead B, Thompson A, Scheven BA, et al. Comparative evaluation of methods for estimating retinal ganglion cell loss in retinal sections and wholemounts. PloS one. 2014;9:e110612. [PubMed: 25343338]
15. Torborg CL, Feller MB. Unbiased analysis of bulk axonal segregation patterns. J Neurosci Methods. 2004;135:17–26. [PubMed: 15020085]
16. Henriksson JT, McDermott AM, Bergmanson JP. Dimensions and morphology of the cornea in three strains of mice. Invest Ophthalmol Vis Sci. 2009;50:3648–3654. [PubMed: 19264894]
17. Pfeiffenberger C, Cutforth T, Woods G, et al. Ephrin-As and neural activity are required for eye-specific patterning during retinogeniculate mapping. Nat Neurosci. 2005;8:1022–1027. [PubMed: 16025107]

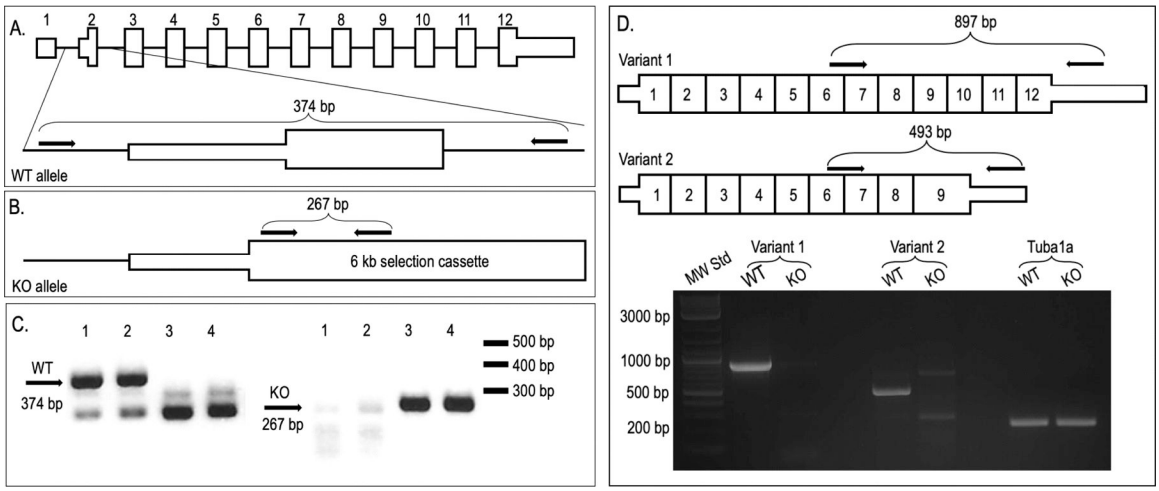

Figure 1.

(A) Schematic depicting the genomic structure of wild-type (WT) *Chrdl1* (not drawn to scale); exon 2, which contains the translation initiation codon, is shown beneath. Arrows indicate the location of PCR primers used for genotyping the WT allele. (B) Schematic depicting the *Chrdl1* knockout (KO) allele (not drawn to scale), in which a 6.3 kb selection cassette is inserted 53 bp into exon 2 but upstream of the translation initiation site. Arrows indicate the location of PCR primers used for genotyping the KO allele. (C) Agarose gel electrophoresis of PCR amplimers used for genotyping 4 male mice, 2 are WT (1 and 2) and 2 are KO (3 and 4). Note, the WT genotyping reaction produces a non-specific amplimer. (D) Schematic depicting 2 *Chrdl1* mRNA variants. Arrows indicate the location of PCR primers used for RT-PCR. Agarose gel electrophoresis of RT-PCR amplimers produced from kidney RNA extracted from male WT and KO mice. Note only WT mouse RNA yields RT-PCR amplimers for the *Chrdl1* variants. Whereas RT-PCR yields amplimers for *Tuba1a* (a positive mRNA control) in WT and KO mice.

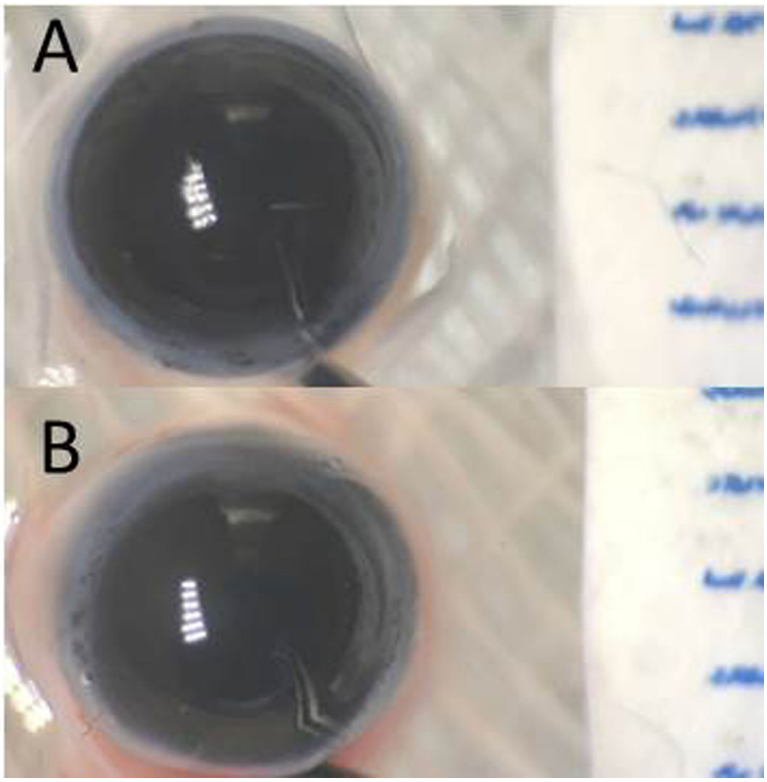

Figure 2.

Eyeballs of WT and KO mice were harvested immediately after euthanasia. (A) shows the right eye of 11-month-old WT mouse; (B) shows the right eye of 10-month-old *Chrdl1* KO mouse. Similar corneal shapes and sizes were found in both eyes.

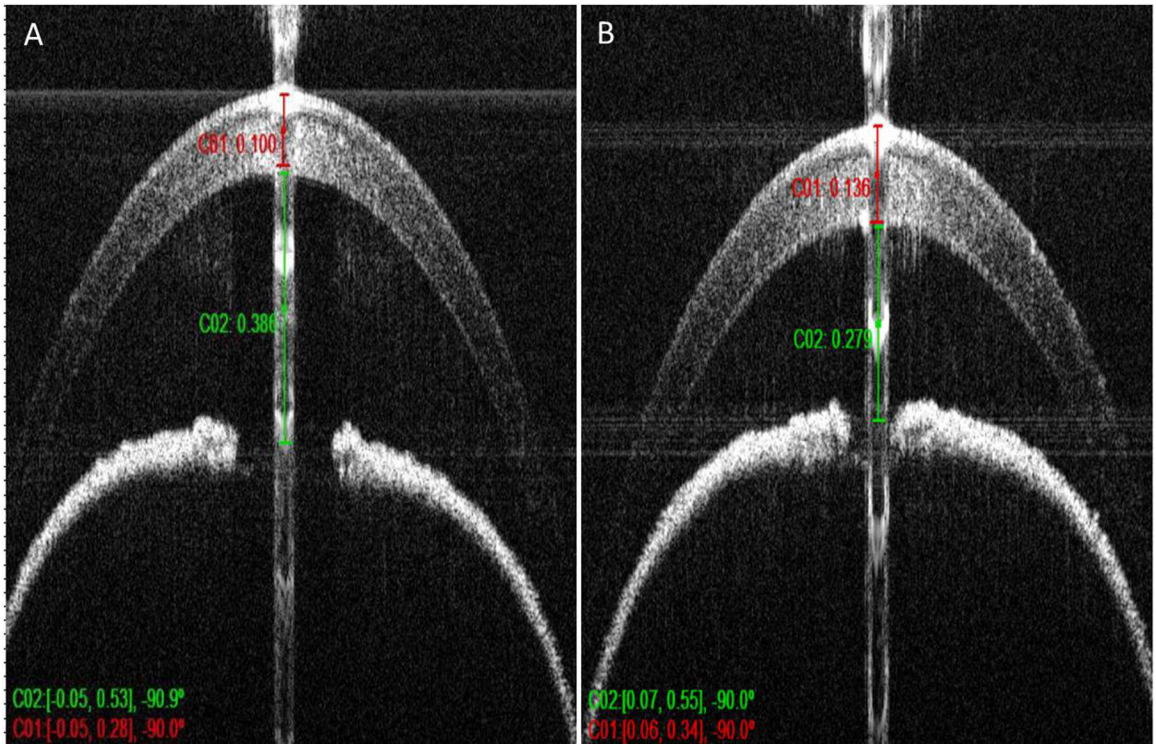

Figure 3.

Representative anterior segment images of WT and KO mice taken by AS-OCT. (A) displays the right eye of a 10-month-old WT mouse; (B) displays the right eye of a 6-month-old KO mouse with a significantly thicker central cornea (red scale bar) and smaller ACD (green scale bar), compared with the WT mice.

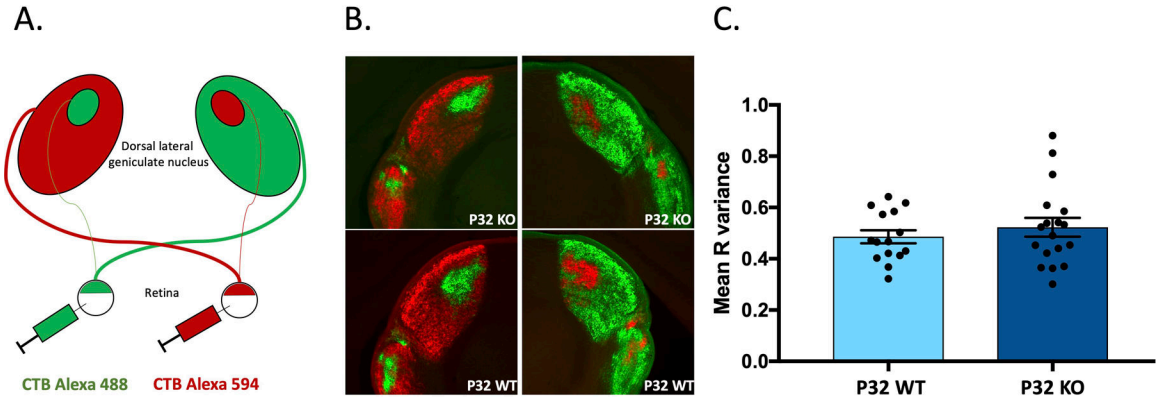

Figure 4.

(A) Schematic for eye injections. Cholera Toxin Subunit B labeled with Alexa 488 or 594 was injected into left or right eye. (B) Representative eye-segregation patterns in dorsal lateral geniculate nucleus (dLGN) of a P32 (4.5-week-old) *Chrdl1* KO mouse *(Top*) and a WT littermate *(Bottom)*. (C) Comparison of the mean R variance between KO and WT shows no significant difference. Mann-Whitney test is performed, $P > 0.05$, n = 15 sections from 3 animals (WT); n = 18 sections from 4 animals (KO), mean ± SEM).

Table 1.

Comparison of ocular parameters between wild type and *Chrdl1* gene knockout mice.

	Wild type (n=14)	**Knockout (n=16)**	***p* value**
Cornea Fluorescein Staining	0 (0 – 4)	0 (0 – 2)	0.4482
Tear Volume (mm)	14.2 ± 1.7	13.2 ± 1.7	0.6672
Intraocular Pressure (mmHg)	30.5 ± 1.1	28.6 ± 1.0	0.2230
Cornea Endothelial Cell Density (cells/mm^2)	1675 ± 26	1662 ± 74	0.8633
Cornea Diameter (mm)	3.13 ± 0.03	3.07 ± 0.05	0.3243
Cornea Area (Arbitrary unit)	7.62 ± 0.13	7.45 ± 0.16	0.4445
Central Cornea Thickness (μm)	100.9 ± 4.2	116.5 ± 3.9	**0.0134***
Anterior Chamber Depth (μm)	405.6 ± 6.3	325.7 ± 5.7	**< 0.0001****
Retinal Ganglion Cell Counts	1079 ± 66	1012 ± 46	0.4497

All data, except for cornea fluorescein staining, are reported as mean ± standard error and comparisons were performed with two-tailed Student's t-tests. The values of cornea fluorescein staining are presented as a median (range) and comparisons were made with Mann-Whitney U test. Significantly greater ($p < 0.05$*) or lower ($p < 0.0001$**) than the value of the opposite group.